

A Study on the Key Factors Determining influence of inorganic ions, organic carbon, and microstructure on the Hygroscopic property of Black Carbon soot

Zhanyu Su^{1,2}, Lanxiadi Chen^{2,3}, Yuan Liu^{1,2}, Peng Zhang¹, Tianzeng Chen¹, Biwu Chu^{1,2}, Mingjin Tang^{2,3}, Qingxin Ma^{1,2*}, Hong He^{1,2}

¹State Key Joint Laboratory of Environment Simulation and Pollution Control, Research Center for Eco-Environmental Sciences, Chinese Academy of Sciences, Beijing 100085, China

²College of Resources and Environment, University of Chinese Academy of Sciences, Beijing 100049, China

³State Key Laboratory of Organic Geochemistry, Guangzhou Institute of Geochemistry, Chinese Academy of Sciences, Guangdong 510640, China

Correspondence to: Qingxin Ma (qxma@rcees.ac.cn)

Abstract. ~~Black carbon (BC) Soot~~ is a crucial component of aerosols in the atmosphere. Understanding the hygroscopicity of ~~BC soot~~ particles is important for studying their role as cloud condensation nuclei (CCN) ~~and ice nuclei (IN)~~, as well as their chemical behavior and atmospheric lifetime. However, there is still a lack of comprehensive understanding regarding the factors that determine the hygroscopic properties of ~~fresh BC soot~~. In this work, the hygroscopic behavior of ~~BC soot~~ particles generated from different types of fuel ~~combustion~~ and aged with SO₂ for varying durations ~~were~~ ~~was~~ measured by a vapor sorption ~~analyzer while various~~ ~~analyser~~. ~~Various~~ characterizations of ~~BC soot~~ were conducted to understand the key factors that influence the hygroscopic properties of ~~BC soot~~. It was found that ~~the presence of~~ water-soluble substances in ~~BC facilitates~~ ~~soot facilitate~~ the completion of monolayer water adsorption at low relative humidity, ~~while also increasing~~ ~~and increase~~ the number of water adsorption layers at high relative humidity. On the other hand, ~~BC soot~~ prepared ~~by~~ ~~from~~ ~~fuels~~ burning ~~organic fuels~~, ~~which~~ typically lacks water-soluble inorganic ions, ~~primarily exhibits~~ ~~and their~~ hygroscopicity ~~characteristics is primarily~~ influenced by organic carbon (OC) and microstructure. Furthermore, the hygroscopicity of ~~BC soot~~ can be enhanced by the formation of sulfate ~~ions~~ due to heterogeneous oxidation of SO₂. ~~This~~ ~~These~~ finding sheds light on the critical factors that affect ~~BC soot~~ hygroscopicity during water adsorption and allows for estimating the interaction between water molecules and ~~BC soot~~ particles in a humid atmosphere. –

30 **Keywords:** ~~black carbon~~soot, hygroscopicity, multilayer adsorption, water-soluble ions, organic carbon, microstructure, heterogeneous reaction

Introduction

~~Black carbon (BC)~~soot particles are produced by incomplete combustion processes of carbon-containing materials (Nie et al., 2020; Wei et al., 2020). ~~The current global emission of BC has been estimated to~~
35 ~~be 3–8 TgC yr⁻¹~~(Petzold et al., 2013). ~~The current global emission of soot has been estimated to be 3–8~~
~~TgC per year~~ (Forster et al., 2007). ~~BC~~soot aerosol can influence climate by directly absorbing solar radiation and affecting cloud formation and surface albedo through deposition on snow and ice (Liao et al., 2015; Peng et al., 2016), which results in the contribution of ~~BC to global warming second only to~~
~~that of CO₂~~(Jacobson, 2001). ~~In addition, BC soot to anthropogenic radiative forcing second only to that~~
40 ~~of CO₂~~ (Bond et al., 2013; Cappa et al., 2012; Liu et al., 2017). ~~In addition, soot~~ particles can significantly enhance the atmospheric oxidation capacity (He et al., 2022) and contribute to the formation of secondary aerosols by providing active surface for the heterogeneous reactions of gaseous pollutants like NO₂, SO₂, and volatile organic compounds (VOCs) (Tritscher et al., 2011; Han et al., 2017; Zhang et al., 2022b; Liu et al., 2023). Moreover, ~~BC~~soot particles also pose a health risk by causing and enhancing respiratory,
45 cardiovascular, and allergic diseases (Janssen et al., 2011; Lin et al., 2011). Due to its significant effect on global climate change, regional air quality and human health, the physicochemical properties of ~~BC~~soot have attracted much attention in recent decades.

Hygroscopicity is one of the most important physicochemical properties of ~~BC~~soot, which largely determines the cloud condensation nuclei (CCN) ~~and ice nucleation (IN)~~ activity as well as the
50 consequent radiation forcing (Semeniuk et al., 2007; Ramanathan and Carmichael, 2008; Friedman et al., 2011). On the other hand, the hygroscopicity of atmospheric particles is important for their chemical behavior because water molecules were found to significantly affect the heterogeneous transformation of gaseous pollutants on ~~BC~~soot surfaces (Zhao et al., 2017; He and He, 2020; Zhang et al., 2022b).–

The hygroscopic behavior of ~~BC~~soot has been widely studied. It was found that ~~fresh BC soot prepared~~
55 ~~in laboratory~~ or commercial ~~BC~~soot appears to be hydrophobic as there is no noticeable uptake of water at unsaturated humidity. For instance, the commercial ~~BC~~soot and spark discharge ~~BC~~soot particles shrunk with increasing RH during the growth factor measurements by hygroscopicity tandem differential

mobility analysers (H-TDMA) (Weingartner et al., 1997; Henning et al., 2010). This was explained with a restructuring of the agglomerated particles. Due to the inverse Kelvin effect, water condenses in small angle cavities of [BCsoot](#) particles, which leads to capillary forces on the branches of the aggregates and cause them to collapse. Different from the commercial [BCsoot](#) and spark discharge [BCsoot](#), diesel [BCsoot](#), aircraft [BCsoot](#) and biomass smoke particle showed obvious particle size growth with increasing RH (Popovicheva et al., 2008; Carrico et al., 2010). This indicates that the chemical composition of [BCsoot](#) is an important factor affecting its hygroscopicity. Our previous study suggested that combustion conditions could affect morphology and microstructure of [BCsoot](#), which has significant effect on the hygroscopicity (Han et al., 2012).

[BCsoot](#) aerosols experience internal mixing with [non-BCother](#) compounds (inorganic, organic, or inorganic/organic mixtures) as aging after their emission (Shiraiwa et al., 2007; Matsui et al., 2013). Field observations have demonstrated that the presence of BC-coating materials greatly influences both the hygroscopic properties and the CCN properties (or the wet removal) (Ohata et al., 2016; Li et al., 2018; Hu et al., 2021). Several laboratory studies have also simulated the hygroscopic changes of [BCsoot](#) particles during atmospheric transport and aging. [BCsoot](#) particles generated from incomplete combustion of propane were exposed to the oxidation products of the OH-toluene reaction, resulting in an organic coating that increased the hygroscopicity of the particles (Qiu et al., 2012). Moreover, the aging process of propane flame [BCsoot](#) through NO₂ oxidation of SO₂ was found to produce inorganic hydrophilic coating materials and significantly enhance the CCN activity of [BCsoot](#) particles (Zhang et al., 2022a).

The hygroscopicity of [BCsoot](#) can vary significantly depending on its source and aging processes, which has implications for regional air quality and climate. However, previous studies have often focused on specific factors influencing the hygroscopicity of a particular type of [BCsoot](#), lacking a comprehensive understanding of the key factors determining the hygroscopic properties of [fresh-BCsoot](#). In this study, we conducted measurements to determine the hygroscopicity of [BCsoot](#) produced from different fuels and aged with SO₂ for different time. In addition, the chemical composition and microstructure of [BCsoot](#) were characterized for each [BCsoot](#) sample. The main objectives of this study were to compare the hygroscopicity of [BCsoot](#) from different sources and analyze the effect of OC, water-soluble ions and microstructure on the multilayer adsorption of [BCsoot](#) surface water. Moreover, the impact of

heterogeneous aging reactions on the multilayer adsorption of water on the surface of BCsoot particles was also explored. This study contributes to a deeper understanding of the hygroscopicity and atmospheric impacts of BCsoot particles in the atmosphere.

90 2. Experimental section

2.1 ~~Black carbon Production.~~ Soot samples.

Prepared BCsoot particles were obtained by burning n-hexane, decane ~~and~~ or toluene (AR, Sinopharm Chemical Reagent Co., Ltd) in a co-flow system as described in our previous studies (Han et al., 2012; Zhao et al., 2017). ~~Diesel black carbon (DBC.~~ Briefly, the co-flow burner consisted of a diffusion flame
95 maintained in a flow of synthetic air. Soot was collected on a quartz disc (7 cm in diameter) over diffusion flame and then stored in a brown bottle (Agilent). Diesel soot (DS) was collected from the diesel particle filter (DPF) of a China VI heavy-duty diesel engine (ISUZU from China). A diesel engine bench test was run under the conditions of World Harmonized Transient Cycle (WHTC). China VI fuels were used in the study, meeting the GB T32859-2016 standard. Printex U ~~black carbon (UBC~~ powder (U-soot) from
100 Degussa (CAS No.: 1333-86-4) was used as a model BCsoot. These types of BCsoots are usually used in laboratory simulation as representative of BCsoot in the atmosphere (Liu et al., 2010; Han et al., 2012; Zhang et al., 2022b).

The aging experiments were performed in a quartz flow tube reactor. ~~UBC~~ Prior to the reaction, 0.05 g U-soot powder was placed into ~~a~~ the quartz flow tube reactor. The experiments were maintained at ~~298~~
105 K25 °C. Zero air was used as the carrier gas, ~~and the~~ with a total flow ~~rate~~ introduced in the flow tube reactor was about 700 ml min⁻¹. The SO₂ concentration was 5 ppm. The relative humidity (RH) was adjusted by varying the ratio of dry zero air to wet zero air at aging reaction was 50 % and measured by a RH sensor ((recorded with Vaisala HMP110). To simulate solar irradiation, a high uniformity integrated xenon lamp (PLS-FX300HU, Beijing Perfectlight Technology Co., Ltd.) of 270 mW cm⁻² was used as
110 the light source. Its visible spectrum ranges from 330 to 850 nm.–

2.2 Characterization of ~~black carbon~~ soot

A transmission electron microscope (H-7500, Hitachi) was used to investigate the morphologies of soot particles. DS sample was ultrasonically dispersed in ethanol while other soot samples were ultrasonically

115 dispersed in ultrapure water (18.2 MΩ cm). Then, a droplet of suspension was deposited onto a Cu microgrid. An acceleration voltage of 200 kV was used for measurements. The diameter of particles was analyzed by ImageJ 1.41 software.

Raman spectra of BCsoots were obtained with a Renishaw inVia Raman microscope system using a 532 nm excitation wavelength. The exposure time for each scan was ~~60s~~60 s. Data were acquired and analyzed using Renishaw WiRE 5.4 software.

120 The content of OC was measured using a thermal-optical transmittance OC/EC analyzer (Sunset laboratory Inc., Forest Grove, OR) with modified NIOSH 5040 protocol and produced four OC fractions (OC1, OC2, OC3, and OC4 at 150, 250, 450, and 550 °C respectively), OP (~~pyrolysed~~pyrolyzed organic) fraction (a pyrolyzed carbonaceous component determined when transmitted laser returned to its original intensity after the sample was exposed to oxygen), and three EC fractions (EC1, EC2, and EC3 at 550,
125 700, and 800 °C, respectively). OC is defined as OC1+OC2+OC3+OC4+OP and EC is defined as EC1+EC2+EC3-OP (Chow et al., 1993; Li et al., 2016).

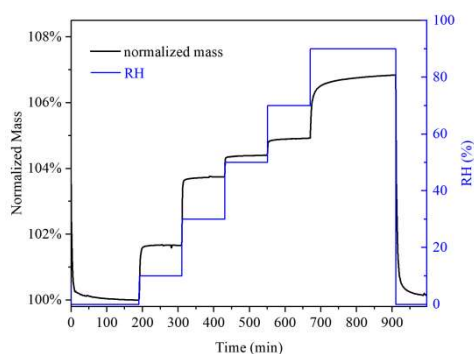
The specieschemical compositions of OC in BCsoots were ~~analyzed and~~ identified via gas chromatography coupled with mass spectrometry (GC-MS, Agilent 6890-5973). 5 mg BCsoot was first ultrasonically extracted for 10 min using 10 ml of dichloromethane (CH₂Cl₂), which was filtered through
130 a quartz sand filter. The obtained supernatant liquid was subsequently concentrated using the N₂ blowing method for final analysis. The gas chromatograph was equipped with a DB-5MS 30 m × 0.25 mm × 0.25 mm capillary column and the mass spectrometer employed a quadrupole mass filter with a ~~70eV~~70 eV electron impact ionizer. The temperature of the programmed temperature vaporizer was held at 270 °C. The initial oven temperature was set at 40 °C for 2 min, then increased step-by-step to 150 °C (by 5 °C
135 min⁻¹) for 5 min, 280 °C (by 10 °C min⁻¹) for 10 min, and 320 °C (by 10 °C min⁻¹) for 5 min.—

For ion chromatography (IC) measurement, about 5 mg of BCsoot particles were extracted by ultrasonication with 10 mL ultrapure water (specific resistance \geq 18.2 MΩ cm) for 10 min. Then, the extract was filtered through a 0.22 μm PTFE membrane filter. The obtained solution was analyzed using a Wayee IC-6200 ion chromatography system equipped with a SI-524E anionic analytical column. An
140 eluent of 10 mM KOH was used at a flow rate of 1.0 mL min⁻¹.

2.3 Hygroscopic properties of ~~black carbon~~soot

The hygroscopic properties of ~~BC~~soots were investigated using a vapor sorption analyzer (VSA, Q5000 SA, TA Instruments), which has been applied to study hygroscopicity of atmospherically relevant particles in previous work (Chen et al., 2019; Gu et al., 2017). VSA utilizes a highly sensitive balance to
145 measure the mass change of a sample as a function of RH at a given temperature. The instrument has a measurement range of 0–100 mg with a sensitivity of 0.01 μg , allowing for precise analysis. The temperature could be controlled in the range of 5–85 $^{\circ}\text{C}$ with an accuracy of 0.1 $^{\circ}\text{C}$, and RH could be regulated in the range of 0–98 % with an absolute accuracy of 1 %. To ensure the accuracy of RH measurements, we routinely measured deliquescence relative humidities (DRHs) of NaCl, $(\text{NH}_4)_2\text{SO}_4$,
150 and KCl, and the difference between measured and theoretical DRHs did not exceed 1 %, confirming the reliability and accuracy of the instrument.

Hygroscopicity of ~~BC~~soot was investigated at ~~298K~~25 $^{\circ}\text{C}$. Figure 1 displays the change of RH and normalized sample mass with experimental time in a typical experiment. ~~UBCU~~soot was dried at $< 1\%$ RH and the sample mass under dry conditions was typically 1–5 mg. After that, RH ~~was~~ increased to
155 ~~90 % start at 10 %~~ step by step, ~~and at~~ from 10 % to 90 %, with an increase of 20 % per step. At each step, RH ~~was~~ increased by 20 %; at each RH point, the ~~sample~~adsorption of water on samples was considered to reach an equilibrium when its mass change was $< 0.05\%$ within 60 min, ~~and then RH was~~ changed to the next value.

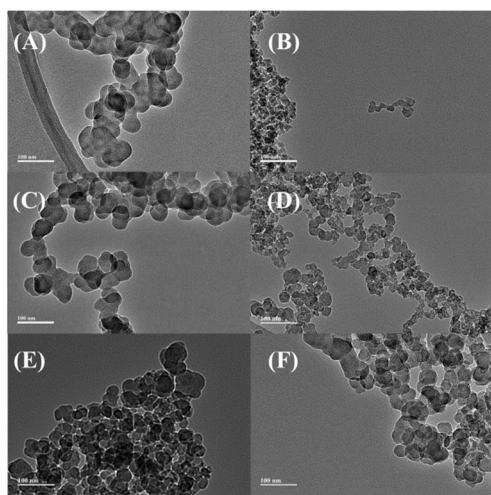


160 **Figure 1.** RH (blue curve, right y axis) and normalized sample mass (black curve, left y axis) as a function of experimental time during one experiment in which hygroscopic properties of ~~UBCU~~soot were examined at ~~298K~~25 $^{\circ}\text{C}$.

3.Result and discussion

3.1The morphology and vapor adsorption isotherms of various black carbon soot

165 Figure 2 shows TEM images of soot samples. All soot samples exhibit a long chain like aggregate shape composed of typical spherical particles, which is consistent with previous studies (Han et al., 2012; Liu et al., 2010).



170 Figure 2. TEM images of n-hexane flame soot (A), decane flame soot (B), toluene flame soot (C), diesel soot (D), U-soot aggregates (E) before and (F) after aged with 5 ppm of SO₂ for 10 h.

Figure 3 shows the diameter distribution of soot particles. Particles exhibit a relatively uniform particle size distribution. Notably, the proportion of spherical particles with large diameter (> 35 nm) of aged U-soot was slightly greater than that of fresh U-soot. Nevertheless, the average particle diameter (\bar{d}_p) of U-soot and SO₂ aged U-soot are 39.55 nm and 41.60 nm, respectively, suggesting weak effect of SO₂
175 heterogeneous reaction on the size distribution of U-soot particles.

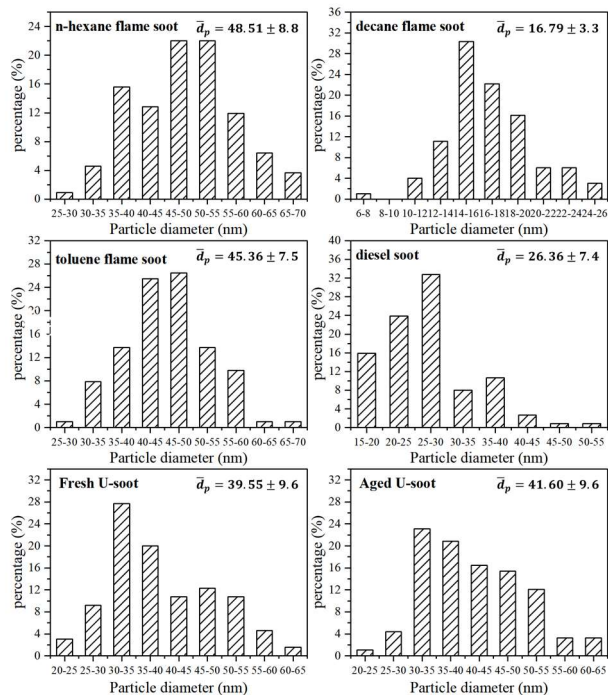


Figure 3. Diameter distribution of n-hexane flame soot, decane flame soot, toluene flame soot and diesel soot and U-soot particles before and after aged with 5 ppm of SO₂ for 10 h.

Figure 4 shows the normalized sample mass (normalized to that at < 1 % RH, m/m_0) as a function of RH for five kindstypes of BCsoot. Three types of prepared BCssoots (n-hexane BCflame soot, decane BCflame soot and toluene BCflame soot) exhibited lower water adsorption per unit mass sample under each RH condition compared to DBCDS and UBCU-soot particles. Specifically, at 90 % RH, DBCDS showed the highest water adsorption of among all BC typessoot samples, with a m/m_0 value of 1.138, followed by UBCU-soot with a value of 1.067. Moreover, among the three prepared BCssoots, decane flame BCsoot exhibited the highest hygroscopicity, as indicated by its with a normalized sample mass of 1.054 at 90 % RH.–

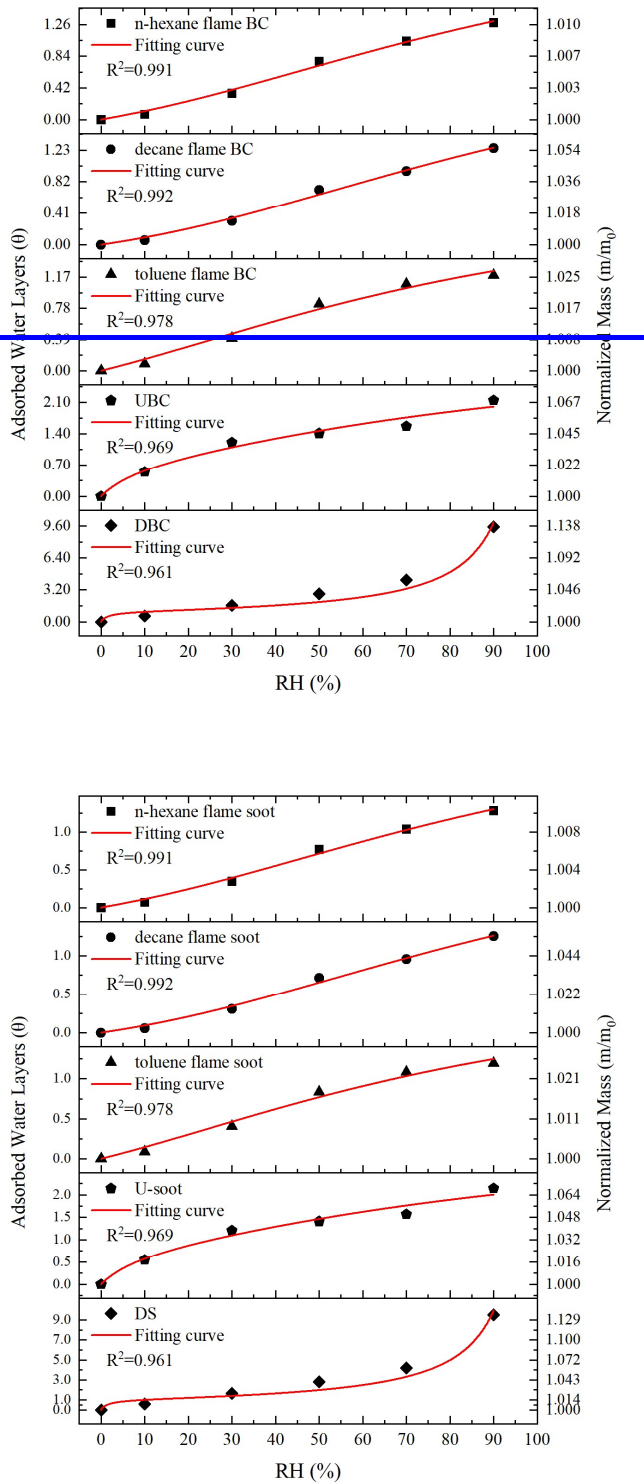


Figure 24. Water adsorption isotherms of **BCs**soots, fitting curves (lines) with BET equation and the measured sample mass change (normalized to that at <1 % RH, i.e., m/m_0) of **BCs**soots as a function of RH (up to 90 % RH).

190

In order to further analyze the adsorption characteristics of water on BCsoot, the isotherms of BCsoot were fitted with the Brunauer-Emmett-Teller (BET) equation. As shown in Fig. 24, the isotherms of prepared BCsoot and UBCU-soot could be well fitted with three-parameters BET equation with the assumption of limited adsorbed water layers as following Eq. (1) (Brunauer et al., 1938; Goodman et al., 2001; Ma et al., 2010; Tang et al., 2016):

$$V = \frac{V_m c \frac{P}{P_0}}{1 - \frac{P}{P_0}} \times \frac{1 - (n+1) \left(\frac{P}{P_0}\right)^n + n \left(\frac{P}{P_0}\right)^{n+1}}{1 + (c-1) \frac{P}{P_0} - c \left(\frac{P}{P_0}\right)^{n+1}} \quad (1)$$

where Where, V is the volume of gas adsorbed at equilibrium pressure P , V_m is the volume of gas necessary to cover the surface of the adsorbent with a complete monolayer, P is the equilibrium pressure of the adsorbing gas, and P_0 is the saturation vapor pressure of the adsorbing gas at that temperature. n is an adjustable parameter given as the maximum number of layers of the adsorbing gas and is related to the pore size and properties of adsorbent. As a result, multilayer formation of adsorbing gas is limited to n layers at large values of P/P_0 . The parameter c is the temperature-dependent constant related to the enthalpies of adsorption of the first and higher layers through Eq. (2) (Brunauer et al., 1938):

$$c = \exp\left(\frac{\Delta H_2^0 - \Delta H_1^0}{RT}\right) \quad (2)$$

where Where, ΔH_1^0 is the standard enthalpy of adsorption of the first layer, and ΔH_2^0 is the standard enthalpy of adsorption on subsequent layers and is taken as the standard enthalpy of condensation, R is the gas constant, and T is the temperature in Kelvin.

For DBCDS, a notable increase in sample mass was observed between 70 % and 90 % RH. This can be attributed to a significant rise in the number of adsorbed water layers within this specific RH range. This hygroscopic characteristic of DBC particles, which leads to an inability to describe the adsorption isotherm that cannot be adequately described by using the three-parameter BET equation, which assumes a limited number of adsorbed water layers. However, the two-parameter BET equation (Eq. (3)), assuming an unlimited number of adsorbed water layers, provides a better fit for the observed adsorption behavior of DBCDS particles (Brunauer et al., 1938):

$$v = \frac{v_m c P}{(p_0 - p)\{1 + (c-1)(p/p_0)\}} \quad V = \frac{V_m c P}{(P_0 - P)\{1 + (c-1)(P/P_0)\}}$$

(3)

The fitted parameters, as shown in Table 1, provide valuable insights into the water adsorption behavior of different **BC_{soot}**. The threshold relative humidity for one monolayer (MRH) for the fresh prepared **BC_{soots}** is approximately 70 % RH. However, both **UBCU-soot** and **DBCDS** exhibit significantly lower MRH values ($MRH_{DBC} = MRH_{DS} = 15\%$, $MRH_{UBC} = 25.5\%$) compared to fresh prepared **BC_{soot}**. This suggests that **UBCU-soot** and **DBCDS** have a higher affinity for water uptake at lower RH levels compared to than fresh **BC_{soot}**. At 90 % RH, prepared **BC_{soot}** and **UBCU-soot** particles were found to have approximately 1.2 and 2.1 layers of surface water adsorbed, respectively. Interestingly, **DBCDS** showed a significantly higher number of surface water layers with around 9.5 layers adsorbed at 90 % RH. This indicates that DBC has, indicating a strong propensity for water adsorption and can accommodate a larger amount of adsorbed water compared to the other BC types.

The water-soluble ions like SO_4^{2-} and NO_3^- in **BC_{soot}** samples were analyzed by IC, and the corresponding results are presented in Table 2. It was observed that the content of NO_3^- in all **BC_{soot}** samples, except for **DBCDS**, was approximately $0.2 \mu g mg^{-1}$. However, **DBCDS** exhibited a higher NO_3^- content of $1.44 \mu g mg^{-1}$, which could be due to the aging of high concentration NO_x coexisting in the exhaust pipe. Regarding SO_4^{2-} , the fresh prepared **BC_{soots}** did not show any detectable levels of SO_4^{2-} . In contrast, both **UBCU-soot** and **DBCDS** displayed notable amounts of SO_4^{2-} , with **UBCU-soot** having a content of $2.54 \mu g mg^{-1}$ and **DBCDS** having the highest content of $11.46 \mu g mg^{-1}$, respectively. These results indicate that water-soluble inorganic ions (e.g., nitrates and sulfates) are dominant factor to enhance for enhancing the hygroscopicity of **BC_{soot}**, which is consistent with previous studies (Carrico et al., 2010; Popovicheva et al., 2010), highlighting the dominance of water soluble inorganic ions in influencing the hygroscopic properties of BC.

Table 1. Adsorption parameters for water uptake on **BC_{soot}.**

Black carbon Soot	BET area ($m^2 g^{-1}$)	MRH (%)	<i>n</i>	<i>c</i>	R^2
n-hexane flame BC_{soot}	26.27	68.0	2.84	1.01	0.991
decane/toluene flame BC_{soot}	70.97/147.36	67.272	2.92/47	0.83/1.37	0.992/978
toluene/decane flame BC_{soot}	147.36/70.97	72.06/7.2	2.47/92	1.37/0.83	0.978/992

<u>DBCDS</u>	47.93	15.0	---	66.95	0.961
<u>UBCU-soot</u>	97.24	25.5	3.34	9.57	0.969
<u>UBCU-soot</u> aged 2h	10.67 <u>99.80</u>	24.4	3.42	10.67	0.973
<u>UBCU-soot</u> aged 6h	9.82 <u>101.46</u>	25.0	3.59	9.82	0.956
<u>UBCU-soot</u> aged 10h	8.52 <u>98.96</u>	26.2	3.82	8.58	0.944

240

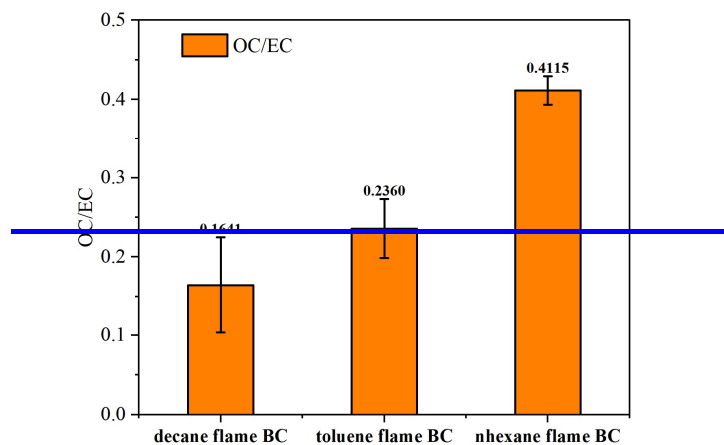
Table 2. Mass concentration of SO₄²⁻ and NO₃⁻ on BCs measured by IC and the ratio of OC/EC of soots.

<u>Black carbon Soot</u>	Mass concentration of	Mass concentration of	<u>OC/EC</u>
	SO ₄ ²⁻ (μg mg ⁻¹)	NO ₃ ⁻ (μg mg ⁻¹)	
n-hexane flame <u>BCsoot</u>	<u>0.00</u>	0.19	<u>0.41±0.02</u>
decane <u>toluene</u> flame <u>BCsoot</u>	<u>0.00</u>	<u>0.18</u>	<u>0.2224±0.04</u>
toluene <u>decane</u> flame <u>BCsoot</u>	<u>0.00</u>	<u>0.22</u>	<u>0.4816±0.06</u>
<u>DBCDS</u>	11.46	1.44	<u>0.14±0.02</u>
<u>UBCU-soot</u>	2.55	0.24	<u>0.12±0.03</u>
<u>UBCU-soot</u> aged 2h	4.83	0.20	---
<u>UBCU-soot</u> aged 6h	7.14	0.19	---
<u>UBCU-soot</u> aged 10h	9.61	0.20	---

3.2 The factors controlling the hygroscopic properties of prepared black carbon soot

Compared with DBCDS and UBCU-soot, prepared BCssoots are more hydrophobic (Fig. 24) due to
 245 less containing fewer water-soluble inorganic ion-contained ions (Table 2). However, there are still
 significant differences in the hygroscopic behavior of BCssoots prepared from different fuels. In order
 to analyze the differences in the hygroscopicity of different prepared BCsoot, the relative content and
 species of OC and microstructure of BCsoot were characterized. Fig. 3 shows the ratio of OC/EC of BC

250 samples. It was found that the n-hexane flame [BC_{soot}](#) has the highest OC/EC ratio, followed by toluene flame [BC_{soot}](#), and decane flame [BC_{soot}](#) has the lowest OC/EC ratio. (Table 2). It should be noted that the ratio of OC/EC is negatively correlated with their hygroscopicity, indicating that organic carbon is not conducive to the adsorption of water on the surface of [BC_{soot}](#). The impact of OC on the hygroscopicity of [BC_{soot}](#) is still a subject of debate. Some field observations results have indicated that particles with high OC/EC ratio were preferentially removed by precipitation and the condensation of photochemically generated secondary organic carbon on [BC_{soot}](#) particles could cause enhancement of hygroscopicity (Dasch and Cadle, 1989; Li et al., 2018). However, HTDMA measurements have shown that neither hygroscopicity nor droplet activation of the fresh propane [BC_{soot}](#) particles depend on the OC content (Henning et al., 2012). Therefore, it is necessary to analyze the specific OC species present in prepared [BC_{soot}](#) particles to gain a better understanding of their role in hygroscopicity.



260

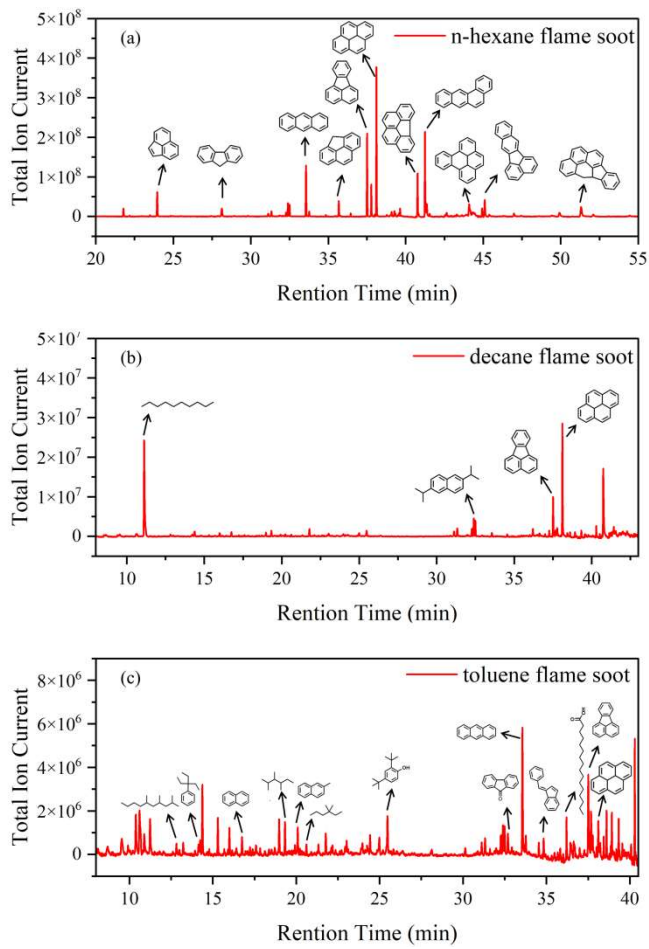
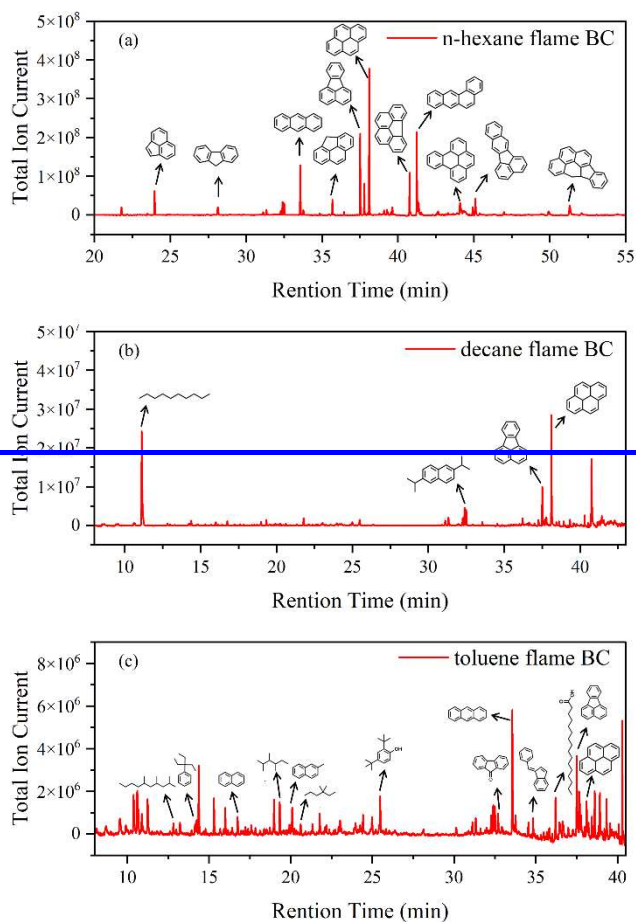


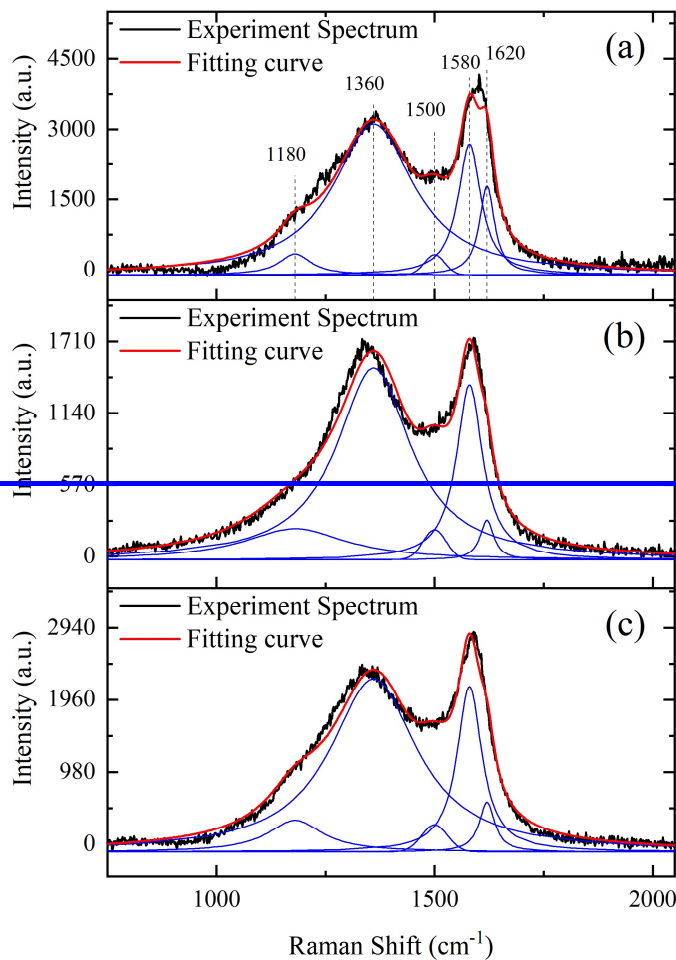
Figure 3. the ratio of $\frac{5OC}{EC}$ of prepared BC measured by a thermal-optical transmittance

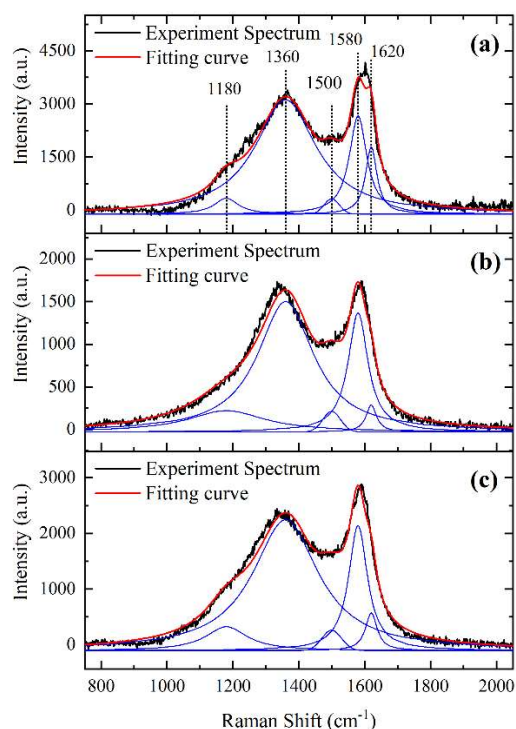


265 **Figure 4.** Total ion chromatogram extracts of prepared **BCsoots**. (a) n-hexane flame **BCsoot**. (b) decane flame **BCsoot**. (c) toluene flame **BCsoot**.

In order to obtain the composition of OC in different **BCsoot**, the samples were extracted by CH_2Cl_2 and the extract was analyzed by GC-MS. **Fig. 4****Figure 5** shows the GC-MS analysis of OC extracted from different prepared **BCsoot**. The major components are polyaromatic hydrocarbons (PAHs) like Anthracene, Fluoranthene and Pyrene in all **BCsoot** samples. It is well known that PAHs are usually
 270 formed simultaneously with **BCsoot** during **prepared combustion**. In n-hexane flame **BCsoot**, PAHs are the main OC while other components are scarce, which is consistent with the results of Han et al. (Han et al., 2012). For decane and toluene flame **BCsoot**, long-chain alkanes such as decane or 2,3,4-trimethylhexane are present in the OC fraction. The characteristic features and peculiarities of the adsorption of water vapor on **BCsoot** are primarily caused by the tendency of polar water molecules to form hydrogen
 275 bonds (Vartapetyan and Voloshchuk, 1995). However, PAHs are weakly polar organic compounds. Thus, the ability of π -electrons in the PAH aromatic ring to form weak hydrogen bonds with water molecules or the interactions with water molecules are either almost absent or are negligible (Lobunez, 1960). The

oxygen-containing functional groups of organic compounds are substantial centers for the formation of hydrogen bonds with water molecules. In toluene flame BC_{soot}, certain OC compounds (2,4-Di-tert-butylphenol, palmitic acid and 9-fluorenone) possess oxygen-containing functional groups like hydroxyl groups, carboxyl groups and quinone. However, these OC compounds also contain substantial hydrophobic parts (aromatic ring and hydrocarbon part). The Despite a small amount, the contribution of these hydrophobic part of a molecule, which is quite small, functional groups to the hygroscopicity is could be dominant (Kireeva et al., 2010). For long-chain alkanes found in decane and toluene flame BC_{soot}, composed solely of carbon and hydrogen atoms soot, they are typically considered hydrophobic. In general, OC constituents detected in these prepared BC_{soot} samples could impede water adsorption on BC_{soot} surfaces. Hence, the presence of these OC compounds leads to hydrophobic characteristics and diminishes the water adsorption capacity of prepared BC_{soot}.





290

Figure 56. Raman spectra of (a) n-hexane, (b) decane and (c) toluene flame **BCsoot**.

In order to study the relationship between the microstructure and vapor adsorption capacity of **BCsoot**, Raman analysis on **BCsoot** samples were conducted. Figure 56 shows the first-order Raman spectra of three prepared **BCsoots** with good curve-fitting results ($R^2 \geq 0.982$), which display well known bands of **BCsoot** near 1580 (G band) and 1360 cm^{-1} (D band). The G band is a typical characteristic of crystalline graphite, while the D band is only observed for disordered graphite. A detailed analysis of the first-order Raman spectra was performed using the five-band fitting procedure proposed by Sadezky (Sadezky et al., 2005). Four Lorentzian-shaped bands (D1, D2, D4, and G, centered at about 1360, 1620, 1180, and 1580 cm^{-1} , respectively) and one Gaussian-shaped band (D3, centered at around 1500 cm^{-1}) were used in the curve-fitting process (Sadezky et al., 2005; Ivleva et al., 2007; Liu et al., 2010). The D1 band arises from the A_{1g} symmetry mode of the disordered graphitic lattice located at the graphene layer edges. The D2 band is attributed to the E_{2g} symmetry stretching mode of the disordered graphitic lattice located at surface graphene layers. The D3 band originates from the amorphous carbon fraction of **BCsoot**. The D4 band is related to the A_{1g} symmetry mode of the disordered graphitic lattice or C–C and C=C stretching vibrations of polyene-like structures, polyenes and ionic impurities also contribute to the D4 band (Sze et al., 2001; Sadezky et al., 2005). The G band is assigned to the ideal graphitic lattice with E_{2g} symmetry vibration mode. The integral intensity ratio (I_D/I_G) of D and G bands could reflect the

295

300

305

comparative content of disordered carbon at graphene layer edges and surface graphene layers, and ~~the~~ was found to be related to the graphite crystallite size L_a (as determined by X-ray) (Knight and White, 1989; Schwan et al., 1996):

$$\frac{44}{L_a} = \left(\frac{I_D}{I_G}\right) \quad (4)$$

The intensities of D and G bands have been widely determined using the sum of D1 and D4 bands and the sum of D2 and G bands. Table 3 shows that the I_D/I_G of three prepared BCs have positive correlation with their hygroscopicity. These results imply that disordered graphitic lattice (D1), graphitic lattice, polyenes, or ionic impurities (D4) could be favorable for the adsorption of water on BC. (Knauer et al., 2009). Table 3 shows similar changing trends between the I_{D4}/I_G of the three prepared soot samples and their hygroscopicity, while the L_a of the three prepared soot samples exhibits a negative correlation. These results imply that disordered graphitic lattice, polyenes, or ionic impurities (D4) could potentially serve as adsorption sites for water molecules. Moreover, graphite crystallite with smaller size could have higher adsorption capacity of water in soot.

Table 3. Parameters I_{D1}/I_G , I_{D2}/I_G , I_{D4}/I_G and I_D/I_G and L_a of n-hexane, decane and toluene flame BCsoot.

Fuels	I_{D1}/I_G	I_{D4}/I_G	$I_{D2}I_D/I_G$	$I_D/I_G L_a(\text{Å})$
n-hexane	$3.822.59 \pm 0.13$	0.4933 ± 0.0201	$2.87 \pm 0.48 \pm 0.0613$	$2.8715.34 \pm 0.1369$
toluene	$3.382.87 \pm 0.0503$	0.5042 ± 0.1109	$3.23 \pm 0.17 \pm 0.0809$	$3.2313.62 \pm 0.0938$
decane	$3.172.69 \pm 0.3008$	0.8575 ± 0.01	$3.49 \pm 0.17 \pm 0.0815$	$3.4912.63 \pm 0.1553$

3.3 The effect of aging process on the hygroscopicity of black carbonsoot.

Based on the hygroscopicity measurements of UBCU-soot and DBCDS (Fig. 24 and 3, Table 2), it is evident that the presence of coating water-soluble inorganic ions (e.g., sulfates and nitrates) can enhance the hygroscopicity of BCsoot particles. Field observations have shown that the mass fractions of ammonium, sulfate, and nitrate increase with the aging of fresh biomass burning particles (Pratt et al., 2011). To investigate the impact of sulfate formation during the aging process on BCsoot hygroscopicity, we aged UBCU-soot with SO₂ for different durations and measured their hygroscopic properties accordingly. The results revealed an increase in sulfate ions on UBCU-soot with longer aging times (Table 2) while the MRH of UBCU-soot remains relatively unchanged with SO₂ aging (Table 1).

However, at 90 % RH, the adsorbed water layers on UBC increases with increasing aging times (Fig. 6). U-soot increases with increasing aging times (Fig. 7). It should be noted that there is a good linear relationship ($R^2 = 0.9997$) between sulfate formed from SO_2 aging and adsorbed water mass at 90 % RH, where a corresponding water absorption mass increase by $1.82\mu\text{g}$ for every $1\mu\text{g}$ of SO_4^{2-} produced on the surface of U-soot.

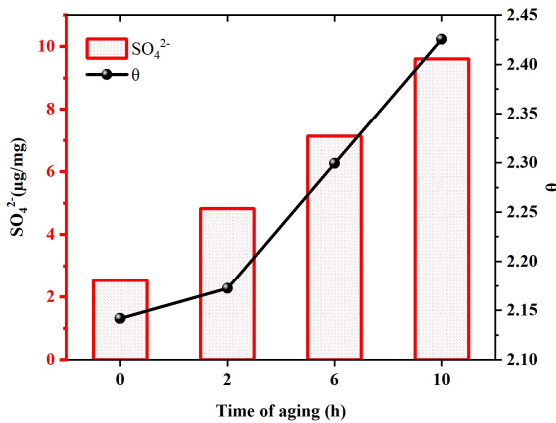


Figure 67. Amounts of sulfates on UBCU-soot and the adsorbed water layers (θ) at 90 % RH of UBCU-soot as a function of the time of aging.

Our previous ~~studies have also indicated~~ study has found that the heterogeneous reaction between SO_2 and BCsoot leads to the formation of sulfuric acid coating on the surface of BCsoot (Zhang et al., 2022b). In this study, the sulfate detected on UBCU-soot could also exist in the form of sulfuric acid. However, IC results demonstrated that the amount of newly generated sulfate on UBCU-soot after ~~42~~10 hours of aging was only 0.706 % of its original mass (Table 2). This small amount is insufficient to cause a significant difference in mass growth at low relative humidity ~~which~~such as cause little change in MRH. However, Kireeva et al. showed that the water adsorption isotherm of graphitized thermal soot coated with a small quantity of sulfuric acid showed a significant increase in the mass growth factor slope of the coated soot at relative humidity levels above 90 % (Kireeva et al., 2010). Zhang et al. found that coating with sulfuric acid could increase the mass growth factor of BCsoot to above 1.2 at 80 % RH relative to fresh particles (Zhang et al., 2008). Our results also demonstrated that a noticeable augmentation in the amount of water adsorbed on SO_2 aged BC ~~at high relative humidity levels~~ soot at 90 % RH, which is positively correlated with the amount of sulfate generated. Based on these findings, it can be concluded that varying amounts of sulfuric acid produced through heterogeneous oxidation on the surface of BC

~~leads~~soot leads to noticeable differences in the amount of adsorbed water at high relative humidity ~~levels~~.

355 These findings are consistent with previous studies ~~demonstrating~~ that coating with sulfuric acid ~~increases~~can increase the hygroscopicity and ice nucleation activation of BCsoot (Demott et al., 1999; Möhler et al., 2005; Wyslouzil et al., 1994).–

4. Conclusion

In this study, we employed a vapor sorption analyzer to investigate the hygroscopicity of BCsoot particles
360 from different sources and at different stages of aging with sulfur dioxide. Multiple characterizations of BCsoot particles were also performed. DBCDS and UBCU-soot contained water-soluble ions, such as sulfates and nitrates, which enabled them to undergo monolayer adsorption at lower relative humidity and increase the number of water absorption layers at higher relative humidity. In contrast, fresh prepared BCsoot particles, which have negligible amounts of water-soluble ions, were more hydrophobic. Their
365 hygroscopicity mainly depended on the organic carbon content and microstructure. ~~A lower~~Lower content of hydrophobic OC and ~~a~~ more disordered graphitic lattice, ~~graphitic lattice~~, polyenes, or ionic impurities made prepared BCsoot particles more prone to water adsorption. The aging of UBCU-soot particles with SO₂ resulted in the formation of water-soluble sulfate ions, which promotes an increase in the hygroscopicity of BCsoot particles. This study analyzed the key factors determining the hygroscopic
370 property of BC, ~~including water soluble ions, organic carbon content, and microstructure. And provides a basis for improving~~soot, which can improve our understanding of the hygroscopic behavior of sulfate-mixed BC in the atmosphere, which couldfresh soot and help to evaluate changes in hygroscopicity during the heterogeneous reactions of BCsoot particles with pollutant gases in future studies. _

375 Data availability

The experimental data are available upon request to the first or corresponding authors

Author Contributions

QM contributed to the conception of the study, ZS and LC designed and conducted this experiment, YL
380 helped to prepare samples. QM, PZ, TC, BC, MT and HH helped perform the analysis with constructive

discussions. ZS and QM wrote the paper with input from all coauthors. All authors contributed to the final paper.

Competing interests

385 The authors declare that they have no conflict of interest.

Acknowledge

This work was supported by the National Key R&D Program of China (2022YFC3701004), and the National Natural Science Foundation of China (No. 22188102), The authors also appreciate the Youth
390 Innovation Promotion Association, CAS (Y2022021).–

Reference

- [Bond, T. C., Doherty, S. J., Fahey, D. W., Forster, P. M., Berntsen, T., DeAngelo, B. J., Flanner, M. G., Ghan, S., Kaercher, B., Koch, D., Kinne, S., Kondo, Y., Quinn, P. K., Sarofim, M. C., Schultz, M. G., Schulz, M., Venkataraman, C., Zhang, H., Zhang, S., Bellouin, N., Guttikunda, S. K., Hopke, P. K., Jacobson, M. Z., Kaiser, J. W., Klimont, Z., Lohmann, U., Schwarz, J. P., Shindell, D., Storelvmo, T., Warren, S. G., and Zender, C. S.: Bounding the role of black carbon in the climate system: A scientific assessment, *Journal of Geophysical Research-Atmospheres*, 118, 5380-5552, 10.1002/jgrd.50171, 2013.](#)
- Brunauer, S., Emmett, P. H., and Teller, E.: Adsorption of gases in multimolecular layers, *Journal of the American Chemical Society*, 60, 309-319, 10.1021/ja01269a023, 1938.
- 400 [Cappa, C. D., Onasch, T. B., Massoli, P., Worsnop, D. R., Bates, T. S., Cross, E. S., Davidovits, P., Hakala, J., Hayden, K. L., Jobson, B. T., Kolesar, K. R., Lack, D. A., Lerner, B. M., Li, S.-M., Mellon, D., Nuaaman, I., Olfert, J. S., Petaja, T., Quinn, P. K., Song, C., Subramanian, R., Williams, E. J., and Zaveri, R. A.: Radiative Absorption Enhancements Due to the Mixing State of Atmospheric Black Carbon, *Science*, 337, 1078-1081, 10.1126/science.1223447, 2012.](#)
- 405 Carrico, C. M., Petters, M. D., Kreidenweis, S. M., Sullivan, A. P., McMeeking, G. R., Levin, E. J. T., Engling, G., Malm, W. C., and Collett, J. L., Jr.: Water uptake and chemical composition of fresh aerosols generated in open burning of biomass, *Atmospheric Chemistry and Physics*, 10, 5165-5178, 10.5194/acp-10-5165-2010, 2010.

- Chen, L., Chen, Y., Chen, L., Gu, W., Peng, C., Luo, S., Song, W., Wang, Z., and Tang, M.: Hygroscopic
410 Properties of 11 Pollen Species in China, *Acs Earth and Space Chemistry*, 3, 2678-2683,
10.1021/acsearthspacechem.9b00268, 2019.
- Chow, J. C., Watson, J. G., Pritchett, L. C., Pierson, W. R., Frazier, C. A., and Purcell, R. G.: THE DRI
THERMAL OPTICAL REFLECTANCE CARBON ANALYSIS SYSTEM - DESCRIPTION,
EVALUATION AND APPLICATIONS IN UNITED-STATES AIR-QUALITY STUDIES,
415 *Atmospheric Environment Part a-General Topics*, 27, 1185-1201, 10.1016/0960-1686(93)90245-t, 1993.
- Dasch, J. M. and Cadle, S. H.: Atmospheric Carbon Particles in the Detroit Urban Area: Wintertime
Sources and Sinks, *Aerosol Science and Technology*, 10, 236-248, 10.1080/02786828908600508, 1989.
- DeMott, P. J., Chen, Y., Kreidenweis, S. M., Rogers, D. C., and Sherman, D. E.: Ice formation by black
carbon particles, *Geophysical Research Letters*, 26, 2429-2432, 10.1029/1999gl900580, 1999.
- 420 Forster, P., Ramaswamy, V., Artaxo, P., Bernsten, T., Betts, R., Fahey, D. W., Haywood, J., Lean, J.,
Lowe, D. C., Myhre, G., Nganga, J., Prinn, R., Raga, G., Schulz, M., and Van Dorland, R.: Changes in
Atmospheric Constituents and in Radiative Forcing, *Ar4 Climate Change 2007: The Physical Science
Basis: Contribution of Working Group I to the Fourth Assessment Report of the Intergovernmental Panel
on Climate Change*, 129-234 pp.2007.
- 425 Friedman, B., Kulkarni, G., Beranek, J., Zelenyuk, A., Thornton, J. A., and Cziczo, D. J.: Ice nucleation
and droplet formation by bare and coated soot particles, *Journal of Geophysical Research-Atmospheres*,
116, D17203, 10.1029/2011jd015999, 2011.
- Goodman, A. L., Bernard, E. T., and Grassian, V. H.: Spectroscopic study of nitric acid and water
adsorption on oxide particles: Enhanced nitric acid uptake kinetics in the presence of adsorbed water,
430 *Journal of Physical Chemistry A*, 105, 6443-6457, 10.1021/jp003722i, 2001.
- Gu, W., Li, Y., Zhu, J., Jia, X., Lin, Q., Zhang, G., Ding, X., Song, W., Bi, X., Wang, X., and Tang, M.:
Investigation of water adsorption and hygroscopicity of atmospherically relevant particles using a
commercial vapor sorption analyzer, *Atmospheric Measurement Techniques*, 10, 3821-3832,
10.5194/amt-10-3821-2017, 2017.
- 435 Han, C., Liu, Y., and He, H.: Heterogeneous reaction of NO(2) with soot at different relative humidity,
Environ Sci Pollut Res Int, 24, 21248-21255, 10.1007/s11356-017-9766-y, 2017.

- Han, C., Liu, Y., Liu, C., Ma, J., and He, H.: Influence of combustion conditions on hydrophilic properties and microstructure of flame soot, *J Phys Chem A*, 116, 4129-4136, 10.1021/jp301041w, 2012.
- He, G., Ma, J., Chu, B., Hu, R., Li, H., Gao, M., Liu, Y., Wang, Y., Ma, Q., Xie, P., Zhang, G., Zeng, X.,
440 C., Francisco, J. S., and He, H.: Generation and Release of OH Radicals from the Reaction of H(2) O with O(2) over Soot, *Angew Chem Int Ed Engl*, 61, e202201638, 10.1002/anie.202201638, 2022.
- He, G. Z. and He, H.: Water Promotes the Oxidation of SO₂ by O₂ over Carbonaceous Aerosols, *Environmental Science & Technology*, 54, 7070-7077, 10.1021/acs.est.0c00021, 2020.
- Henning, S., Ziese, M., Kiselev, A., Saathoff, H., Moehler, O., Mentel, T. F., Buchholz, A., Spindler, C.,
445 Michaud, V., Monier, M., Sellegri, K., and Stratmann, F.: Hygroscopic growth and droplet activation of soot particles: uncoated, succinic or sulfuric acid coated, *Atmospheric Chemistry and Physics*, 12, 4525-4537, 10.5194/acp-12-4525-2012, 2012.
- Henning, S., Wex, H., Hennig, T., Kiselev, A., Snider, J. R., Rose, D., Dusek, U., Frank, G. P., Pöschl, U., Kristensson, A., Bilde, M., Tillmann, R., Kiendler-Scharr, A., Mentel, T. F., Walter, S., Schneider,
450 J., Wennrich, C., and Stratmann, F.: Soluble mass, hygroscopic growth, and droplet activation of coated soot particles during LACIS Experiment in November (LExNo), *Journal of Geophysical Research-Atmospheres*, 115, D11206, 10.1029/2009jd012626, 2010.
- Hu, D., Wang, Y., Yu, C., Xie, Q., Yue, S., Shang, D., Fang, X., Joshi, R., Liu, D., Allan, J., Wu, Z., Hu, M., Fu, P., and McFiggans, G.: Vertical profile of particle hygroscopicity and CCN effectiveness during
455 winter in Beijing: insight into the hygroscopicity transition threshold of black carbon, *Faraday Discuss*, 226, 239-254, 10.1039/d0fd00077a, 2021.
- Ivleva, N. P., Messerer, A., Yang, X., Niessner, R., and Poeschl, U.: Raman microspectroscopic analysis of changes in the chemical structure and reactivity of soot in a diesel exhaust aftertreatment model system, *Environmental Science & Technology*, 41, 3702-3707, 10.1021/es0612448, 2007.
- 460 [Jacobson, M. Z.: Strong radiative heating due to the mixing state of black carbon in atmospheric aerosols, *Nature*, 409, 695-697, 10.1038/35055518, 2001.](#)
- Janssen, N. A. H., Hoek, G., Simic-Lawson, M., Fischer, P., van Bree, L., ten Brink, H., Keuken, M., Atkinson, R. W., Anderson, H. R., Brunekreef, B., and Cassee, F. R.: Black Carbon as an Additional Indicator of the Adverse Health Effects of Airborne Particles Compared with PM₁₀ and PM_{2.5},
465 *Environmental Health Perspectives*, 119, 1691-1699, 10.1289/ehp.1003369, 2011.

- Kireeva, E. D., Popovicheva, O. B., Khokhlova, T. D., and Shoniya, N. K.: Laboratory simulation of the interaction of water molecules with carbonaceous aerosols in the atmosphere, *Moscow University Physics Bulletin*, 65, 510-515, 10.3103/s0027134910060159, 2010.
- 470 [Knauer, M., Schuster, M. E., Su, D. S., Schlögl, R., Niessner, R., and Ivleva, N. P.: Soot Structure and Reactivity Analysis by Raman Microspectroscopy, Temperature-Programmed Oxidation, and High-Resolution Transmission Electron Microscopy, *Journal of Physical Chemistry A*, 113, 13871-13880, 10.1021/jp905639d, 2009.](#)
- [Knight, D. S. and White, W. B.: Characterization of diamond films by Raman spectroscopy, *Journal of Materials Research*, 4, 385-393, 10.1557/JMR.1989.0385, 1989.](#)
- 475 Li, C., Hu, Y., Chen, J., Ma, Z., Ye, X., Yang, X., Wang, L., Wang, X., and Mellouki, A.: Physiochemical properties of carbonaceous aerosol from agricultural residue burning: Density, volatility, and hygroscopicity, *Atmospheric Environment*, 140, 94-105, 10.1016/j.atmosenv.2016.05.052, 2016.
- Li, K., Ye, X., Pang, H., Lu, X., Chen, H., Wang, X., Yang, X., Chen, J., and Chen, Y.: Temporal variations in the hygroscopicity and mixing state of black carbon aerosols in a polluted megacity area, *Atmospheric Chemistry and Physics*, 18, 15201-15218, 10.5194/acp-18-15201-2018, 2018.
- 480 Liao, H., Chang, W., and Yang, Y.: Climatic Effects of Air Pollutants over China: A Review, *Advances in Atmospheric Sciences*, 32, 115-139, 10.1007/s00376-014-0013-x, 2015.
- Lin, W., Huang, W., Zhu, T., Hu, M., Brunekreef, B., Zhang, Y., Liu, X., Cheng, H., Gehring, U., Li, C., and Tang, X.: Acute Respiratory Inflammation in Children and Black Carbon in Ambient Air before and during the 2008 Beijing Olympics, *Environmental Health Perspectives*, 119, 1507-1512, 10.1289/ehp.1103461, 2011.
- 490 [Liu, D., Whitehead, J., Alfarra, M. R., Reyes-Villegas, E., Spracklen, D. V., Reddington, C. L., Kong, S., Williams, P. I., Ting, Y.-C., Haslett, S., Taylor, J. W., Flynn, M. J., Morgan, W. T., McFiggans, G., Coe, H., and Allan, J. D.: Black-carbon absorption enhancement in the atmosphere determined by particle mixing state, *Nature Geoscience*, 10, 184-U132, 10.1038/ngeo2901, 2017.](#)
- [Liu, Y., He, G., Chu, B., Ma, Q., and He, H.: Atmospheric heterogeneous reactions on soot: A review, *Fundamental Research*, 3, 579-591, <https://doi.org/10.1016/j.fmre.2022.02.012><https://doi.org/10.1016/j.fmre.2022.02.012>, 2023.](#)

Liu, Y., Liu, C., Ma, J., Ma, Q., and He, H.: Structural and hygroscopic changes of soot during
495 heterogeneous reaction with O₃, *Physical Chemistry Chemical Physics*, 12, 10896-10903,
10.1039/c0cp00402b, 2010.

Lobunez, W.: Book Reviews : The Hydrogen Bond. , *Textile Research Journal*, 30, 1006-1007,
10.1177/004051756003001217, 1960.

Ma, Q., He, H., and Liu, Y.: In situ DRIFTS study of hygroscopic behavior of mineral aerosol, *Journal*
500 *of Environmental Sciences*, 22, 555-560, 10.1016/s1001-0742(09)60145-5, 2010.

Matsui, H., Koike, M., Kondo, Y., Moteki, N., Fast, J. D., and Zaveri, R. A.: Development and validation
of a black carbon mixing state resolved three-dimensional model: Aging processes and radiative impact,
Journal of Geophysical Research: Atmospheres, 118, 2304-2326, 10.1029/2012jd018446, 2013.

Möhler, O., Büttner, S., Linke, C., Schnaiter, M., Saathoff, H., Stetzer, O., Wagner, R., Krämer, M.,
505 Mangold, A., Ebert, V., and Schurath, U.: Effect of sulfuric acid coating on heterogeneous ice nucleation
by soot aerosol particles, *Journal of Geophysical Research*, 110, D11210, 10.1029/2004jd005169, 2005.

~~[Nie, B., Peng, C., Wang, K., and Yang, L.: Structure and Formation Mechanism of Methane Explosion
Soot, *Acs Omega*, 5, 31716-31723, 10.1021/acsomega.0c04234, 2020.](#)~~

Ohata, S., Schwarz, J. P., Moteki, N., Koike, M., Takami, A., and Kondo, Y.: Hygroscopicity of materials
510 internally mixed with black carbon measured in Tokyo, *Journal of Geophysical Research: Atmospheres*,
121, 362-381, 10.1002/2015jd024153, 2016.

Peng, J., Hu, M., Guo, S., Du, Z., Zheng, J., Shang, D., Zamora, M. L., Zeng, L., Shao, M., Wu, Y.-S.,
Zheng, J., Wang, Y., Glen, C. R., Collins, D. R., Molina, M. J., and Zhang, R.: Markedly enhanced
absorption and direct radiative forcing of black carbon under polluted urban environments, *Proceedings*
515 *of the National Academy of Sciences of the United States of America*, 113, 4266-4271,
10.1073/pnas.1602310113, 2016.

~~[Petzold, A., Ogren, J. A., Fiebig, M., Laj, P., Li, S. M., Baltensperger, U., Holzer-Popp, T., Kinne, S.,
Pappalardo, G., Sugimoto, N., Wehli, C., Wiedensohler, A., and Zhang, X. Y.: Recommendations for
reporting "black carbon" measurements, *Atmospheric Chemistry and Physics*, 13, 8365-8379,
520 \[10.5194/acp-13-8365-2013\]\(#\), 2013.](#)~~

- Popovicheva, O., Persiantseva, N. M., Shonija, N. K., DeMott, P., Koehler, K., Petters, M., Kreidenweis, S., Tishkova, V., Demirdjian, B., and Suzanne, J.: Water interaction with hydrophobic and hydrophilic soot particles, *Physical Chemistry Chemical Physics*, 10, 2332-2344, 10.1039/b718944n, 2008.
- Popovicheva, O. B., Kireeva, E. D., Timofeev, M. A., Shonija, N. K., and Mogil'nikov, V. P.:
525 Carbonaceous aerosols of aviation and shipping emissions, *Izvestiya Atmospheric and Oceanic Physics*, 46, 339-346, 10.1134/s0001433810030072, 2010.
- Pratt, K. A., Murphy, S. M., Subramanian, R., DeMott, P. J., Kok, G. L., Campos, T., Rogers, D. C., Prenni, A. J., Heymsfield, A. J., Seinfeld, J. H., and Prather, K. A.: Flight-based chemical characterization of biomass burning aerosols within two prescribed burn smoke plumes, *Atmospheric Chemistry and*
530 *Physics*, 11, 12549-12565, 10.5194/acp-11-12549-2011, 2011.
- Qiu, C., Khalizov, A. F., and Zhang, R.: Soot Aging from OH-Initiated Oxidation of Toluene, *Environmental Science & Technology*, 46, 9464-9472, 10.1021/es301883y, 2012.
- Ramanathan, V. and Carmichael, G.: Global and regional climate changes due to black carbon, *Nature Geoscience*, 1, 221-227, 10.1038/ngeo156, 2008.
- 535 Sadezky, A., Muckenhuber, H., Grothe, H., Niessner, R., and Pöschl, U.: Raman micro spectroscopy of soot and related carbonaceous materials: Spectral analysis and structural information, *Carbon*, 43, 1731-1742, 10.1016/j.carbon.2005.02.018, 2005.
- [Schwan, J., Ulrich, S., Batori, V., Ehrhardt, H., and Silva, S. R. P.: Raman spectroscopy on amorphous carbon films. *Journal of Applied Physics*, 80, 440-447, 10.1063/1.362745, 1996.](#)
- 540 Semeniuk, T. A., Wise, M. E., Martin, S. T., Russell, L. M., and Buseck, P. R.: Hygroscopic behavior of aerosol particles from biomass fires using environmental transmission electron microscopy, *Journal of Atmospheric Chemistry*, 56, 259-273, 10.1007/s10874-006-9055-5, 2007.
- Shiraiwa, M., Kondo, Y., Moteki, N., Takegawa, N., Miyazaki, Y., and Blake, D. R.: Evolution of mixing state of black carbon in polluted air from Tokyo, *Geophysical Research Letters*, 34, L16803,
545 10.1029/2007gl029819, 2007.
- Sze, S. K., Siddique, N., Sloan, J. J., and Escribano, R.: Raman spectroscopic characterization of carbonaceous aerosols, *Atmospheric Environment*, 35, 561-568, 10.1016/s1352-2310(00)00325-3, 2001.

Tang, M., Cziczo, D. J., and Grassian, V. H.: Interactions of Water with Mineral Dust Aerosol: Water Adsorption, Hygroscopicity, Cloud Condensation, and Ice Nucleation, *Chemical Reviews*, 116, 4205-550 4259, 10.1021/acs.chemrev.5b00529, 2016.

Tritscher, T., Juranyi, Z., Martin, M., Chirico, R., Gysel, M., Heringa, M. F., DeCarlo, P. F., Sierau, B., Prevot, A. S. H., Weingartner, E., and Baltensperger, U.: Changes of hygroscopicity and morphology during ageing of diesel soot, *Environmental Research Letters*, 6, 034026, 10.1088/1748-9326/6/3/034026, 2011.

555 Vartapetyan, R. S. and Voloshchuk, A. M.: Adsorption mechanism of water molecules on carbon adsorbents, *Uspekhi Khimii*, 64, 1055-1072, 1995.

~~[Wei, X., Zhu, Y., Hu, J., Liu, C., Ge, X., Guo, S., Liu, D., Liao, H., and Wang, H.: Recent Progress in Impacts of Mixing State on Optical Properties of Black Carbon Aerosol, *Current Pollution Reports*, 6, 380-398, 10.1007/s40726-020-00158-0, 2020.](#)~~

560 Weingartner, E., Burtscher, H., and Baltensperger, U.: Hygroscopic properties of carbon and diesel soot particles, *Atmospheric Environment*, 31, 2311-2327, 10.1016/s1352-2310(97)00023-x, 1997.

Wyslouzil, B. E., Carleton, K. L., Sonnenfroh, D. M., Rawlins, W. T., and Arnold, S.: OBSERVATION OF HYDRATION OF SINGLE, MODIFIED CARBON AEROSOLS, *Geophysical Research Letters*, 21, 2107-2110, 10.1029/94gl01588, 1994.

565 Zhang, F., Peng, J., Chen, L., Collins, D., Li, Y., Jiang, S., Liu, J., and Zhang, R.: The effect of black carbon aging from NO₂ oxidation of SO₂ on its morphology, optical and hygroscopic properties, *Environmental Research*, 212, 113238, 10.1016/j.envres.2022.113238, 2022a.

Zhang, P., Chen, T., Ma, Q., Chu, B., Wang, Y., Mu, Y., Yu, Y., and He, H.: Diesel soot photooxidation enhances the heterogeneous formation of H₂SO₄, *Nat Commun*, 13, 5364, 10.1038/s41467-022-570 33120-3, 2022b.

Zhang, R., Khalizov, A. F., Pagels, J., Zhang, D., Xue, H., and McMurry, P. H.: Variability in morphology, hygroscopicity, and optical properties of soot aerosols during atmospheric processing, *Proceedings of the National Academy of Sciences of the United States of America*, 105, 10291-10296, 10.1073/pnas.0804860105, 2008.

575 Zhao, Y., Liu, Y., Ma, J., Ma, Q., and He, H.: Heterogeneous reaction of SO₂ with soot: The roles of relative humidity and surface composition of soot in surface sulfate formation, *Atmospheric Environment*, 152, 465-476, [10.1016/j.atmosenv.2017.01.005](https://doi.org/10.1016/j.atmosenv.2017.01.005), 2017.